A&A 416, 759–764 (2004)
DOI: 10.1051/0004-6361:20034341

Astronomy & Astrophysics

Evidence for magnetic reconnection in the high corona

G. M. Simnett⋆

School of Physics and Astronomy, University of Birmingham, B15 2TT, UK

Received 17 September 2003 / Accepted 5 November 2003

Abstract. The LASCO C2 coronagraph on the SOHO spacecraft shows many examples of oppositely-directed mass flows along the same (projected) radius vector. We have analysed 40 such events to understand their origin and possible physical cause. The events all had the speed of the outflowing feature higher than that of the inflowing feature. This is interpreted as reflecting an energy release in the outflowing solar wind. 19 of the 40 events had speed differences between 75 and 165 km s^{-1}, with the median speed difference being 112 km s^{-1}. One consequence of this is that the typical solar wind speed at the site of the event onset is around 60 km s^{-1}. Back projection of the altitude-time plots gives an estimate of the height in the corona of the originating event. For 38 of the 40 events this (projected) height is between 3.1 and 4.2 solar radii. One plausible interpretation of the physical mechanism responsible for the events is magnetic reconnection as first described by Petschek (1964).

Key words. Sun: corona – Sun: magnetic fields

1. Introduction

The low solar corona is a tenuous magnetised plasma, dominated at low latitudes by closed magnetic structures. The extent of the closed structures is probably dependent on the phase of the solar cycle, with more at solar maximum. It is also likely that they extend to high latitudes at solar maximum. The footpoints of the structures emerge through the photosphere, and are therefore continually being driven by photospheric motion. One possible outcome of these motions is magnetic reconnection, which would also release energy in the corona. Such a possibility has been discussed by Petschek (1964) in connection with the energy release mechanism for solar flares.

There is another reason to suspect that reconnection may be taking place quasi-continuously in the high corona. Fisk (1996) suggested a modification to the simple Parker spiral magnetic field to recognise the fact that the corona rotates almost as a rigid body, whereas the photosphere exhibits significant differential rotation. This must result in some shear interface at moderately high latitudes. Furthermore, from direct measurements over a wide range of altitudes, Lewis et al. (1999) showed that the high corona rotated slightly slower than that below around 2 $R_\odot$, and therefore there must be a shear interface near 2 $R_\odot$.

Energetic particle observations near 1 AU show that non-thermal solar electrons in the energy range up to 10–20 keV are frequently present. Lin (1985) has drawn attention to the fact that the energy spectrum for 2–20 keV impulsive electron bursts continues as an unbroken power law down to below 2 keV, which implies that the electrons have passed through very little material since their acceleration. Lin pointed out that these small impulsive electron events are the most common type of event occurring on the Sun. This suggests a process occurring in the high corona, at least above a Sun-centred altitude of ~2 $R_\odot$, which is releasing energy and accelerating the electrons.

These results suggest that transient energy releases should be occurring in the high corona. Thus we have searched the LASCO C2 coronagraph data set for evidence that energy release might be occurring in the region above 2 $R_\odot$.

2. The observations

The observations were made with the LASCO C2 coronagraph (Brueckner et al. 1995) on the SOHO spacecraft. This coronagraph detects photospheric light in the optical region of the spectrum which has been Thomson-scattered off free electrons in the corona. It has a circular, Sun-centred field-of-view from approximately 2 $R_\odot$ to 6 $R_\odot$. The instrument is suited to detect mass changes in the corona, as typically each free electron has an associated nucleon. The most sensitive measurements are made via running difference images, where the image being viewed has had the previous image subtracted from it. In this way, regions of the corona that have experienced a mass increase show as white, and regions that have experienced a mass decrease show as black. In practice a greyscale colour table is used to provide a graded image covering degrees of white or black.

Detailed examination of the LASCO data revealed features that moved both inwards and outwards along a radius vector. Examples of these phenomena were published by Simnett (2000) for events on 5 May, 1999 and 23 October, 1999, and Wang et al. (1999b) for events on 7 September, 1996 and 17 May, 1998. Figure 1 shows another event from 6 November,

⋆ e-mail: gms@star.sr.bham.ac.uk

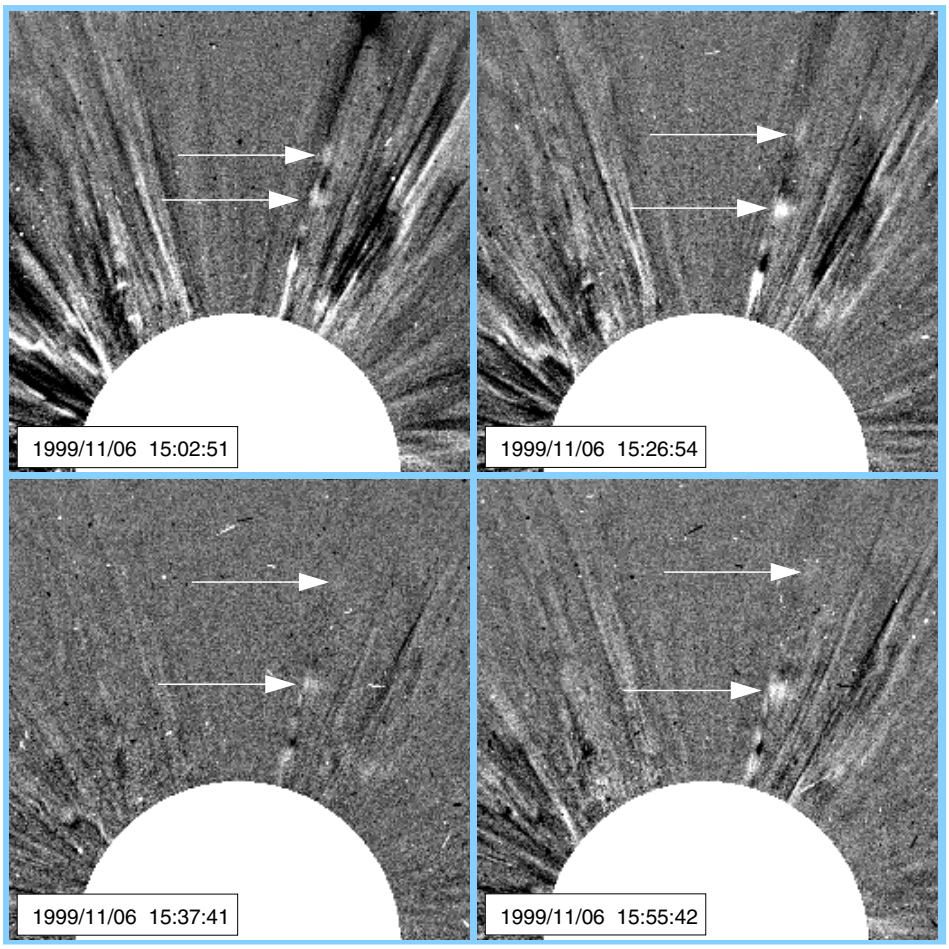

Fig. 1. Running difference images from the LASCO C2 coronagraph for the bidirectional event on 6 November, 1999. The outflowing and inflowing material flows are indicated by the arrows.

1999. The time of each image is given in the lower left corner of each frame. The white semicircle represents half of the solar occulting disc with the boundary at 2.2 $R_{\odot}$. North is at the top of each frame and west to the right. In this paper we refer to features in terms of their position angle, PA, which is the polar angle in degrees measured anticlockwise from the origin at the north pole. The features we discuss in Fig. 1 are at a position angle ~345°.

In the first two images the corona is clearly relatively dynamic, with many changes, especially when compared with the image at 15:37:41 UT. We draw attention to two blobs, indicated by arrows in each frame. For this event, the feature moving outwards is relatively faint compared to the feature moving inwards. It should be noted that in each frame the features are actually a pair of white/black blobs, with the black being at a larger radius behind the inward moving feature, and at a smaller radius for the outward moving feature. The sequence is best viewed as a movie.

Figure 2 shows an event from 10 April, 2000. Here only the southwest quadrant of the field-of-view is shown. The sequence of images is in the same format as Fig. 1, as for Fig. 3. Here the outward feature clearly has a width of approximately 10°, and it is seen easiest in the dark arc, although each dark arc has a faint bright arc at a larger radial distance. It appears as though the part of the arc at the smaller position angle, i.e. closer to the south pole, is connected to a narrow, dark radial feature, which is probably a streamer. The two ends of each arc point back to the Sun and the inward moving feature, indicated by the upper arrow in each frame, is associated with just one end.

Figure 3 gives an example of an event on 8 May, 1999 which we regard as close to the threshold level of detectability. The inward moving feature is best seen as the small concentrated black blob, while the outward feature is quite diffuse. We have searched the LASCO data for similar events and this paper is a report on the first 40 events discovered. A list of the events, in chronological order, is given in Table 1. The primary selection criteria were that the radius vector of the mass motions be the same, within the angular width of the events, and that the event be visible as both an inflow and an outflow in several consecutive images.

There are several quantitative parameters which may be evaluated for each event. The first two are the speed of the inflowing and outflowing features. These are estimated from the height-time plots of the features, and are in the plane of the sky. Therefore they are lower limits, but are probably accurate to 10%. The estimate of the accuracy is derived from the fact that sec 20° = 1.064, and that a large fraction of the events seen by LASCO is within 20°–30° off the plane of the sky.

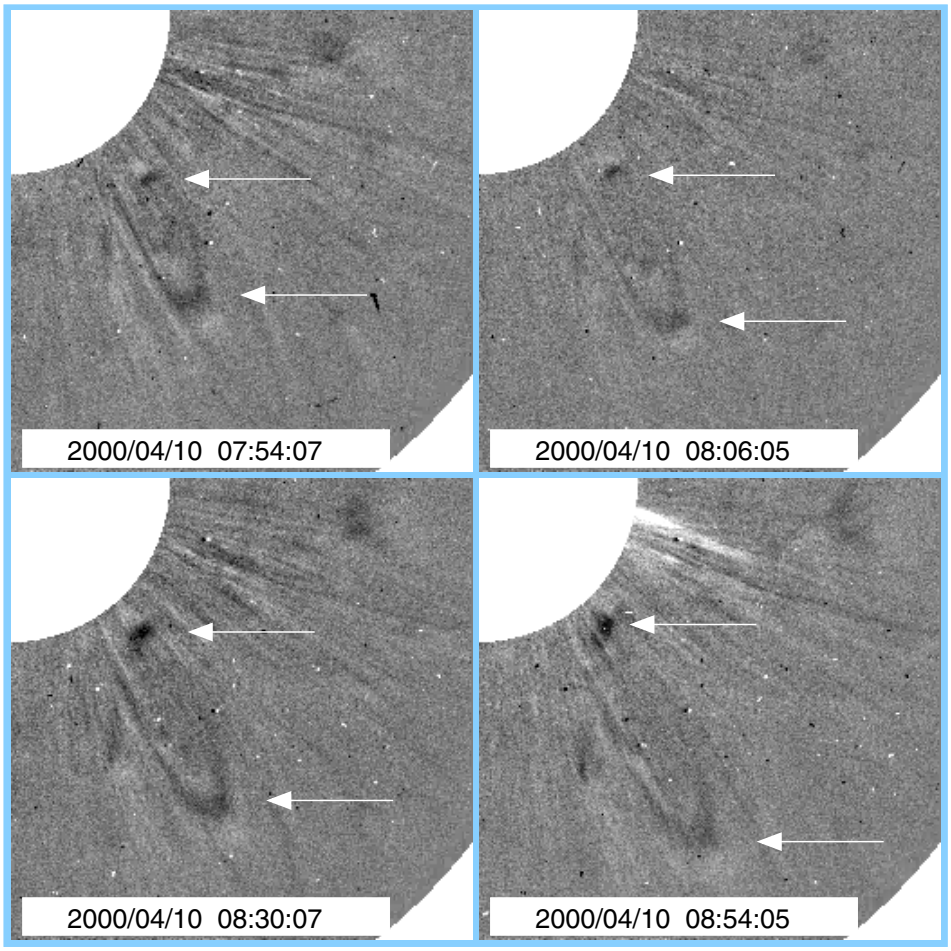

Fig. 2. Running difference images from the LASCO C2 coronagraph for the bidirectional event on 10 April, 2000. The outflowing and inflowing material flows are indicated by the arrows.

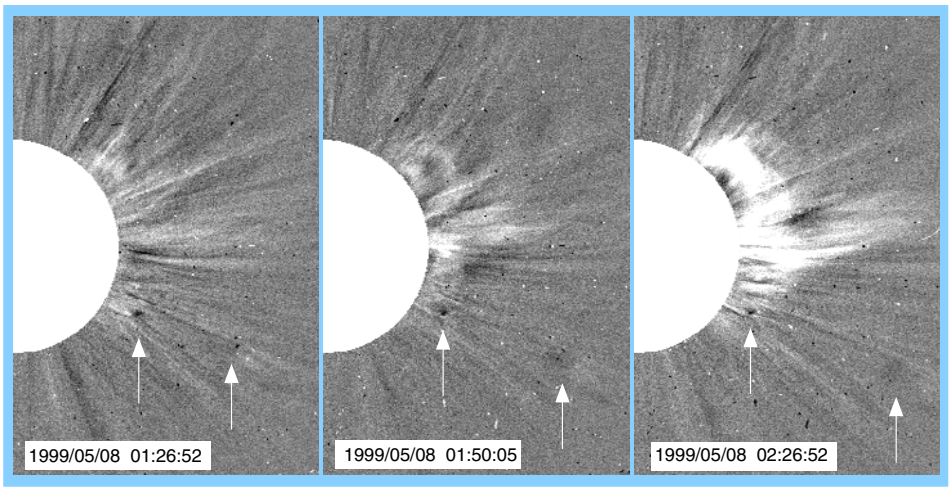

Fig. 3. Running difference images from the LASCO C2 coronagraph for the bidirectional event on 8 May, 1999. The outflowing and inflowing material flows are indicated by the arrows.

Figure 4 shows the height-time plots for four events from the list. In general all the features we have studied have constant projected speed, with no obvious acceleration or deceleration. All events we have found have the speed of the outflow greater than the speed of the inflow, and the speed difference is given in the fourth column of Table 1. As the events all have uniform speeds, within the accuracy of the measurements, it is possible to extrapolate the height-time plots backwards in time to provide an intercept height. This is given in Col. 5 and is a lower limit as the events are projected onto the plane of the sky.

Table 1. The bidirectional events.

Date	Speed In km s^{-1}	Speed Out km s^{-1}	Out-In km s^{-1}	Intercept Height $R_\odot$	PA °	Starting Time (UT)	Type III
5 May 1998	79	144	65	4.2	345	14:27	nd
1 April 1999	151	212	61	3.3	238	18:37	nd
5 May 1999	118	259	141	3.2	65	07:55	N
8 May 1999	28	174	146	3.3	242	00:30	nd
11 May 1999	52	175	123	3.5	238	16:12	Y
12 May 1999	79	191	112	3.4	240	01:45	Y
12 May 1999	55	274	219	4.2	238	09:55	N
27 May 1999	100	265	165	3.7	302	07:48	?
21 June 1999	43	189	146	3.8	222	21:55	Y
25 June 1999	44	164	120	3.4	222	13:55	?
5 Aug. 1999	98	364	266	4.1	141	00:59	N
7 Oct. 1999	62	91	29	3.9	77	03:55	N
22 Oct. 1999	73	159	86	3.4	172	23:10	N
30 Oct. 1999	130	190	60	3.8	258	13:30	N
31 Oct. 1999	52	248	196	2.7	265	06:45	Y
2 Nov. 1999	79	159	80	4.2	5	02:30	N
3 Nov. 1999	64	109	45	4.9	37	15:15	Y
6 Nov. 1999	79	144	65	4.2	345	14:27	N
4 Jan. 2000	114	125	11	3.1	217	09:45	N
24 Jan. 2000	169	230	61	3.6	86	03:25	N
5 Feb. 2000	123	199	76	4.4	235	22:30	N
11 Feb. 2000	42	226	184	3.7	144	17:30	Y
24 Feb. 2000	97	217	120	3.7	78	03:19	Y
3 March 2000	79	370	191	3.2	135	16:15	?
4 March 2000	155	239	84	3.5	239	10:08	Y
16 March 2000	145	330	185	3.3	295	19:08	Y
1 April 2000	90	118	28	4.0	344	18:35	N
10 April 2000	86	189	103	3.5	214	06:30	Y
10 April 2000	114	176	28	4.2	354	12:10	N
10 April 2000	81	296	215	3.6	210	17:52	N
29 April 2000	83	212	129	4.1	267	09:38	Y
13 May 2000	64	95	31	3.4	293	05:20	N
14 May 2000	90	302	212	3.8	242	19:15	Y
24 May 2000	77	254	177	3.9	209	12:20	Y
14 Jan. 2001	84	171	87	3.6	283	14:00	N
14 Jan. 2001	62	150	88	3.3	231	20:58	?
16 March 2001	85	259	174	3.4	224	07:00	N
25 Jan. 2002	44	191	147	3.7	58	05:15	N
25 Jan. 2002	73	177	104	3.7	291	10:55	Y
10 Nov. 2002	120	281	161	3.8	290	06:19	Y

We have given in Col. 6 the approximate position angle of the event. This is accurate to approximately 3°, and in the case of wide events, such as those shown in Fig. 2 and by Simnett (2000) the PA for centre of the event is given. There is a bias towards the western hemisphere, and more specifically towards the southwest. This is not regarded as significant; it is probably partly due to statistics, and partly to the way in which we scanned the LASCO data, which possibly introduced an observer bias. The LASCO data were not interrogated systematically, but on a quasi-random basis, and many of the events were detected while surveying the data for other purposes. Nevertheless we need to address the frequency of the bidirectional events. This has been achieved by a careful search of all the data for the four month period 1 February–31 May, 2000, when 15 events were detected, which results in a frequency of slightly less than 1/week.

To study whether there is any association between the bidirectional events and the impulsive electron events discussed in the introduction, we have searched the WIND/WAVES data (Courtesy: Dr M. L. Kaiser, Goddard Space Flight Center, MD, USA) for evidence of decametric type III radio emission at the projected starting time. The time of the intercepts (see, for example, those in Fig. 4) is given in Col. 7 in Table 1. We estimate that these have a maximum uncertainty of around +/−30 min.

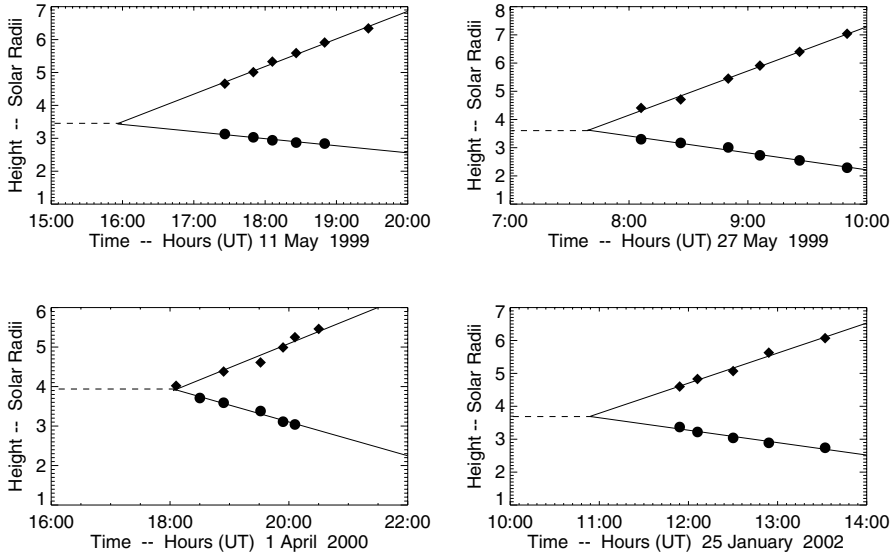

Fig. 4. Height-time plots for the bidirectional events on 11 May, 1999; 27 May, 1999; 1 April, 2000 and 25 January, 2002. The dashed horizontal line corresponds to the estimated height of the initiating event.

In the final column of Table 1 we simply list as Y(es) or N(o) according to whether there was a type III burst or not, within this time envelope. Out of the 40 events, 7 occurred either at times of no data(3) or during a noise storm(4); 15 had a type III burst association, and 18 had no type III burst association. Given that plasma radiation should not propagate to the WIND spacecraft from behind the plane of the sky which includes the Sun (the reference plane), one might expect half the events with correlated radio emission to be Y in Table 1, and half to be N. The LASCO events should, statistically, come equally from behind and in front of the reference plane. Thus the observed association of the WIND type III events with the bidirectional events is *consistent* with there being electron acceleration associated with all of them. However, note that this is just a consistency check.

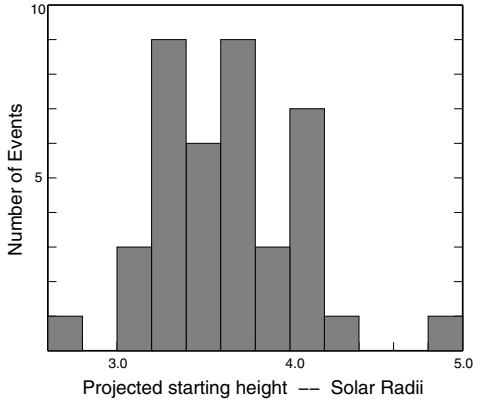

Fig. 5. The distribution of projected starting heights in the corona.

3. Discussion

We have plotted in Fig. 5 a histogram of the projected starting heights from Col. 5 in Table 1. Given the uncertainty of the projection, we have binned the data in units of 0.2 $R_\odot$. 38 of the 40 events appear to start between 3.1 and 4.4 $R_\odot$, with one at 2.7 $R_\odot$ and one at 4.9 $R_\odot$. More than half the events lie between 3.3 and 3.8 $R_\odot$.

We now address in more detail the way in which the events were detected. Most of the material observed by LASCO is flowing away from the Sun; therefore there are many small jets and blobs moving outwards. There are, however, frequent small events observed to move inwards (Wang et al. 1999a; Sheeley & Wang 2000). These typically form at heliocentric distances of ~3–5 $R_\odot$. We started our search by selecting first those blobs that moved inwards. As pointed out by Wang et al. inflows are not detected to start outside of 5 $R_\odot$ either because they are not present there, or because they are too faint to be seen. Thus the apparent upper limit may be real, or may be a threshold effect. However, the outflows that we have detected in conjunction with an inflow are typically able to be tracked beyond 6 $R_\odot$ (see Fig. 4) so we believe the upper cut-off to the starting height is real.

The apparent cut-off at the lower side is almost certainly real. We have stated above that we have used the detection of an inflow as a search criterion; such inflows are readily seen below 3 $R_\odot$, and so the lack of bidirectional events below 3 $R_\odot$ is not due to lack of visibility.

A histogram of the difference between the inflow and outflow speeds is shown in Fig. 6. All the outflow speeds are higher than the inflow speeds, and 19 out of 40 lie between 75 and 165 km s^{-1} (see Table 1).

The origin of the bidirectional events is interpreted as follows. We suggest that the evidence supports the hypothesis postulated in the Introduction that the events represent energy release from reconnecting magnetic fields, similar to the suggestion of Petschek (1964). With any form of energy release via reconnection, the magnetic Reynolds number is critical. In the corona, as in most astrophysical situations, the magnetic Reynolds number is very large, such that diffusive reconnection is very slow. The advance made by Petschek was to recognise that the reconnection is speeded up by the effects of wave

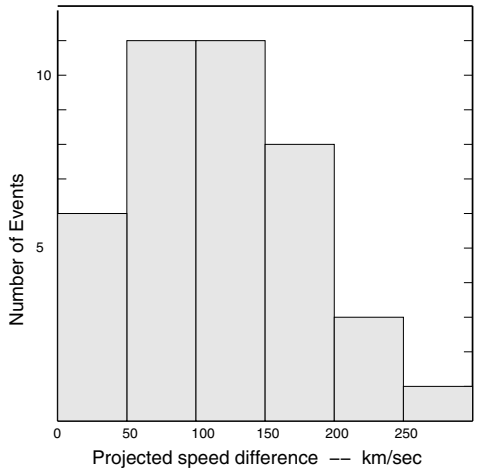

Fig. 6. The distribution of projected speed differences between the outflow and inflow.

propagation, which may be thought of as going at the local Alfvén speed. It is beyond the scope of this paper to discuss this further, but we regard it significant that the Petschek-type reconnection is aided by the presence of a high Alfvén speed.

Mann et al. (2003) have drawn attention to the fact that the local Alfvén speed reaches a maximum in the corona at around 3.8 $R_\odot$. This is precisely where the conditions most favorable to Petschek reconnection would occur.

If we then adopt as a working hypothesis that this is what is happening, we can investigate the physical conditions pertinent to the reconnection site. First, if the reconnection is occurring in an outward flowing fluid, namely the solar wind, then the solar wind speed at the reconnection site is half the observed speed difference. If we take the typical height of a bidirectional event as 3.7 $R_\odot$, which is the median value from the 40 events in Table 1, and couple that with the median speed difference of 112 km s^{-1}, then we would obtain a "typical" solar wind speed of 56 km s^{-1}. To allow for the obvious uncertainties involved in this estimate, and for projection effects, a more appropriate speed would be ~60 km s^{-1}.

The solar wind speed inferred from the continuous outflows seen by LASCO at this altitude is around 40–50 km s^{-1} (Tappin et al. 1999). The typical speed of discrete blobs measured by Sheeley et al. (1997) at this altitude, is around 100 km s^{-1}. Both these values are near the low altitude limit of the observations, and as such are subject to considerable uncertainty, at least enough to be compatible with our estimate from the bidirectional events.

We finally discuss the frequency of the events. During the four-month period of comprehensive scrutiny, events were detected at the rate of around 1/week. An event such as shown in Fig. 2 is visible only because the coronagraph is looking along the propagating front of the event. In this instance the front has a curvature. A front is two dimensional, and the events which are detected as blobs are presumably events where the line of sight is 90° away from this direction, but still looking along the front. If the observer is looking at any other angle, then the event would not be detected. Thus for an event to be detected, the observing geometry has to be at a precise orientation. It is plausible that only ~1% of events are detectable.

We now return to the question of energetic electron acceleration. If the reconnection is as we have postulated, then there will be shocks propagating both outwards and inwards. We would expect such shocks to accelerate energetic particles, and we further suggest that these events are the coronal source of the impulsive low energy electron events reviewed by Lin (1985). The decametric type III burst association lends some support to this.

4. Conclusions

The main result of this work is the identification of bidirectional mass flows in the corona. The identified features move in and out along the same radius vector, which was one of the selection criteria. The events are interpreted as explosive energy release in the outflowing solar wind at regions where there is magnetic reconnection. If this interpretation is correct, then these events represent the first direct observation of magnetic reconnection in the corona. A typical altitude for the initiation of the events is around 3.7 $R_\odot$, which is close to the altitude of the maximum Alfvén speed in the corona (Mann et al. 2003). If the reconnection is via the Petschek mechanism, then this would be expected. The outflowing material is always moving faster than the inflowing material. From this a typical inferred average solar wind speed at 3.7 $R_\odot$ of ~60 km s^{-1} is derived.

Acknowledgements. The author wishes to thank members of the LASCO Consortium for their advice and encouragement. Starlink computing facilities were used for the analysis of the data.

References

Brueckner, G. E., Howard, R. A., Koomen, M. J., et al. 1995, Sol. Phys., 162, 357
Fisk, L. A. 1996, J. Geophys. Res., 101, 15, 547
Lewis, D. J., Simnett, G. M., Brueckner, G. E., et al. 1999, Sol. Phys., 184, 297
Lin, R. P. 1985, Sol. Phys., 200, 58
Mann, G., Klassen, A., Aurass, H., & Classen, H.-T. 2003, A&A, 400, 329
Petschek, H. E. 1964, in Physics of Solar Flares, ed. W. N. Hess, NASA SP-50, 425
Simnett, G. M. 2000, Astron. Soc. Pacific Conf. Ser., ed. R. Ramaty, & N. Mandzhavidze, 206, 43
Sheeley, N. R. Jr., Wang, Y.-M., Hawley, S. H., et al. 1997, ApJ, 484, 472
Sheeley, N. R. Jr, & Wang, Y.-M. 2001, ApJ, 562, L107
Tappin, S. J., Simnett, G. M., & Lyons, M. A. 1999, A&A, 350, 302
Wang, Y.-M., Sheeley, N. R. Jr., Howard, R. A., St. Cyr, O. C., & Simnett, G. M. 1999a, Geophys. Res. Lett., 26, 1203
Wang, Y.-M., Sheeley, N. R. Jr., Howard, R. A., Rich, N. B., & Lamy, P. L. 1999b, Geophys. Res. Lett., 26, 1349